

Article

From Memristor-Modeled Jerk System to the Nonlinear Systems with Memristor

Xianming Wu ¹, Shaobo He ^{2,*}, Weijie Tan ³ and Huihai Wang ²

¹ School of Mechanical & Electrical Engineering, Guizhou Normal University, Guiyang 550001, China; jsdxwxm@126.com

² School of Physics and Electronics, Central South University, Changsha 410083, China; wanghuihai_csu@csu.edu.cn

³ State Key Laboratory of Public Big Data, Guizhou University, Guiyang 550025, China; wjtian@gzu.edu.cn

* Correspondence: heshabo@csu.edu.cn

Abstract: Based on the proposed generalized memristor, a new jerk system is proposed. The complex dynamics of the system are investigated by means of bifurcation diagrams, Lyapunov exponents, and MSampEn, and rich dynamics are observed. Moreover, the circuits of the generalized memristor and the jerk system are physically implemented in the hardware level. The experimental results show that the memristor circuit can generate “8”-shaped pinched hysteresis loops, and the observed attractors match well with the numerical simulations results. In this paper, we summarize nonlinear systems with memristors in the references. It indicates that there are two symmetry methods to find a memristor model in nonlinear systems. However, some of them cannot be realized using the memristor devices, although a memristor model can be found. For example, the famous Lorenz system contains a memristor function, but it cannot be realized using the memristor device. The principles regarding whether nonlinear systems with a memristor function can be realized using a memristor device are discussed.

Keywords: jerk system; memristor; chaos; complexity; symmetry



Citation: Wu, X.; He, S.; Tan, W.; Wang, H. From Memristor-Modeled Jerk System to the Nonlinear Systems with Memristor. *Symmetry* **2021**, *14*, 659. <https://doi.org/10.3390/sym14040659>

Academic Editor: Antonio Palacios

Received: 22 February 2022

Accepted: 22 March 2022

Published: 24 March 2022

Publisher's Note: MDPI stays neutral with regard to jurisdictional claims in published maps and institutional affiliations.



Copyright: © 2020 by the authors. Licensee MDPI, Basel, Switzerland. This article is an open access article distributed under the terms and conditions of the Creative Commons Attribution (CC BY) license (<https://creativecommons.org/licenses/by/4.0/>).

1. Introduction

In 1971, the concept of the memristor was proposed by Chua [1], and it indicates that the new element is the fourth basic circuit electron element, while the other three are resistor, capacitor, and inductance. Then, in 1976, memristive devices and systems with memristors were investigated [2]. However, the research regarding the memristor did not develop very far until 2008. In this year, a nanoscale TiO₂ device that provides a method for the physical realization of the memristor was reported by Strukov et al. [3]. Since then, memristor performance has been simulated using the differential operator, and the memristor simulators have been widely investigated and used in many different research fields, such as nonlinear systems [4,5], storage [6], synapses [7], and neural networks [8]. Unlike the continuous memristors mentioned above, discrete memristors are designed based on the difference operator. The discrete memristor can be used to model the discrete chaotic maps. For instance, the Hénon map and Sine map are designed and investigated [9,10].

The jerk system is one of the simplest nonlinear systems for chaos. For instance, a jerk system can be defined as [11]:

$$\frac{d^3x}{dt^3} + \beta \frac{d^2x}{dt^2} + \alpha \frac{dx}{dt} = f(x), \quad (1)$$

where $f(\cdot)$ is a nonlinear function. Since $f(\cdot)$ has different choices and those jerk systems have complex dynamical behaviors, it has attracted lots of research interest [12–15]. For instance, multistability has been found when the system has different nonlinear functions

and an image encryption application is carried out. Based on the memristor function, jerk systems with memristors can be designed, and relevant studies can be found in Refs. [16–19]. Generally speaking, the generalized memristor uses one of the equations in the jerk system and the memristor function is set in the nonlinear function $f(\cdot)$. Although there are many nonlinear systems with memristors, it is still interesting to investigate how to introduce a memristor in nonlinear systems. Since jerk systems are a recent hot topic [20], the generalized memristors in a jerk system is investigated. Moreover, it is necessary to analyze complex dynamics of the designed system [21]. There are two methods to realize circuits of the memristor chaotic system. The first method is to use the memristor module, while the second method is to realize the system based on the equations, since those circuits in the present research are complicated, and since it is necessary to investigate how to reduce electron components in the memristor-based jerk system. Finally, the conception of a memristor chaotic system should be clear. Some of the systems are designed based on the memristor, while the others only contain memristor functions. At present, the circuit realization of different nonlinear chaotic systems is a hot topic [22], and the theory of how to design circuits for nonlinear systems based on memristive devices deserves further study. Thus, we need to figure out what is a real memristor chaotic system and discuss the difference between a “memristor chaotic system” and a “chaotic system with memristor function”.

Motivated by the above discussions, in this paper, a third-order jerk system with a generalized memristor is designed. The dynamics of the system are analyzed by means of bifurcation diagrams and Lyapunov exponents (LEs). Meanwhile, the complexity of the time series from the system is investigated by the multiscale SampEn (MSampEn) [23], and circuit implementation of the system is carried out. Since it has already been indicated that the nonlinear systems including the jerk system can contain memristors, we further investigate those systems with memristors and try to summarize the rules behind them. The rest of this paper is organized as follows. In Section 2, a generalized memristor is proposed and a jerk system is designed based on the memristor. In Section 3, the dynamics of the jerk system with memristors are investigated numerically, and the circuits for the generalized memristor and the jerk system are designed and realized in the hardware circuit. In Section 4, a discussion on the relationship between the generalized memristor and nonlinear systems is carried out. Section 5 is the summary.

2. The Generalized Memristor-Based Jerk System

2.1. The Generalized Memristor

Chua et al. [2] proposed the concept of the generalized memristor, and it is defined by:

$$\begin{cases} y(t) = g(x, h, t)h(t) \\ \dot{x}(t) = f(x, h, t) \end{cases}, \quad (2)$$

where $h(t)$ and $y(t)$ are the input and output of the memristor, respectively. x is the internal state of the memristor, which is defined by the differential equation. Later, Adhikari et al. [24] defined the memristor as:

$$\begin{cases} v = M(x_1, x_2, \dots, x_n)i \\ \dot{x}_k = f_k(x_1, x_2, \dots, x_n; i), \end{cases} \quad (3)$$

where $M(\cdot)$ is the memristor function called memristance, x_n are the state variables, i is the current, and $f(\cdot)$ is the associated state equation. Meanwhile, they investigated the three fingerprints of the memristors.

Secondly, according to the definition of generalized memristor, we propose a generalized memristor, which is defined by:

$$\begin{cases} h = e(x-1)y \\ \dot{x} = y \end{cases}, \quad (4)$$

where h represents the output of the memristor, which can be the voltage (current), y is the current (voltage), and x is the internal state variable of the memristive element, which can be the electromagnetism (charge).

Suppose that the input of the memristor is given by:

$$y(t) = A \sin(2\pi ft), \quad (5)$$

then, the internal state variable of the memristor is calculated by:

$$\begin{aligned} x(t) &= \int_{-\infty}^t y(\tau) d\tau \\ &= \int_{-\infty}^0 y(\tau) d\tau + \int_0^t y(\tau) d\tau, \\ &= x(t_0) + \frac{A}{2\pi f} [1 - \cos(2\pi ft)] \end{aligned} \quad (6)$$

and the output of the memristor is denoted as:

$$\begin{aligned} h(t) &= e(x - 1)y \\ &= A \left[x(t_0) + \frac{A}{2\pi f} (1 - \cos(2\pi ft)) - 1 \right] \sin(2\pi ft). \end{aligned} \quad (7)$$

Here, $x(t_0)$ is the initial condition of the generalized memristor.

Let $A = 1$, $f = 0.2$, $f = 0.5$, and $f = 1$; the input ($y(t)$) and output ($h(t)$) of the memristor are shown in Figure 1a. Fix $f = 0.2$, $A = 1$, $A = 2$, and $A = 4$; the input ($y(t)$) and output ($h(t)$) of the memristor are illustrated in Figure 1b. It shows in Figure 1 that the proposed generalized memristor shows typical “8”-shaped hysteresis curves. When the frequency of the input signal increases, the internal area of the hysteresis curves decreases. As a result, it shows that the designed electronic device is a generalized memristor.

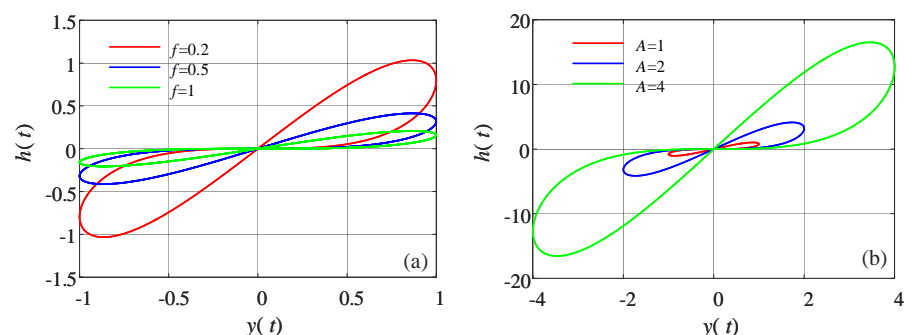


Figure 1. Relationship curves of the input and output of the generalized memristor. (a) $A = 1$, $f = 0.2$, $f = 0.5$, and $f = 1$; (b) $f = 0.2$, $A = 1$, $A = 2$, and $A = 4$.

2.2. Model of the Jerk System with Memristor

A three-dimensional jerk system can be described by the following equations [11]:

$$\begin{cases} \dot{x} = y \\ \dot{y} = z \\ \dot{z} = -bx - ey - cz + f(x) \end{cases}, \quad (8)$$

where x , y , and z are state variables, $f(x)$ is the nonlinear function, and b , c , and e are the positive real numbers. By introducing the proposed memristor to this system, we designed a new jerk system, which can be defined as:

$$\begin{cases} \dot{x} = y \\ \dot{y} = z \\ \dot{z} = -bx - cz + e(x - 1)y \end{cases}, \quad (9)$$

where x , y , and z are state variables. Obviously, $f(x) = exy$, and the system contains the generalized memristor as proposed in the above section.

For the proposed system, the volume shrinkage ratio is denoted as:

$$\nabla V = \frac{\partial \dot{x}}{\partial x} + \frac{\partial \dot{y}}{\partial y} + \frac{\partial \dot{z}}{\partial z} = -c; \quad (10)$$

then, $V(t) = V(0)e^{-ct}$. When $c > 0$, it can be found that the proposed system is a dissipative system, and it converges to zero or the domain of attraction with a speed of e^{-ct} .

The equilibrium point of system (9) is $(x_0, y_0, z_0) = (0, 0, 0)$; thus, the Jacobian matrix at the equilibrium point is:

$$J_E = \begin{bmatrix} 0 & 1 & 0 \\ 0 & 0 & 1 \\ -b & -e & -c \end{bmatrix}. \quad (11)$$

Its characteristic polynomial is denoted as:

$$|\lambda I - J_E| = \lambda^3 + c\lambda^2 + e\lambda + b = 0. \quad (12)$$

According to the Routh–Hurwitz criterion, if the real part of all the roots is negative, then the equilibrium point is stable; otherwise, the equilibrium point is unstable. When $c > 0$, $b > 0$, $ce - b > 0$, the characteristic equation has three negative real-part roots; thus, the system is stable. When $c > 0$, $b > 0$, $ce - b < 0$, the zero equilibrium point is a saddle node; accordingly, the equilibrium point is unstable. Specifically, suppose that $c = 1$, $b = 1$; then, the value of the parameter e should be smaller than one.

3. Dynamics and Circuit Implementation

There are three parameters in the system, namely, b , c , and e . Since the parameter e belongs to the memristor, we fix it as $e = 0.5$ and investigate the complex dynamics of the system with the variation of b and c . In this paper, bifurcation diagrams, Lyapunov exponents (LEs), phase diagrams, and multiscale SampEn are employed to analyze the complex dynamics of the system.

3.1. Dynamical Behaviours

3.1.1. Bifurcation Analysis

Fix $c = 1$, $e = 0.5$ and vary b from 0.4 to 1, with a step size of 0.0024. A bifurcation diagram and its corresponding LEs are shown in Figure 2. This shows that the jerk system enters chaos with period-doubling bifurcation. When $b > 0.88$, the system becomes too chaotic and the corresponding maximum Lyapunov exponents are larger than zero. The phase diagrams of the system, with $c = 1$, $e = 0.5$, and different b , including $b = 0.7$, $b = 0.818$, $b = 0.88$, and $b = 1$, are illustrated in Figure 3. It shows that there are periodically one, periodically two, and periodically four circles with symmetrical structures and chaotic attractors, and it also shows the period-doubling bifurcation of the system with the increase of the parameter b .

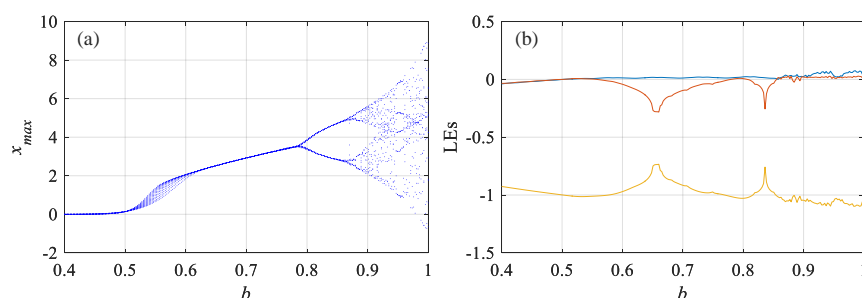


Figure 2. Dynamics of the memristor-based jerk system with the parameter b . (a) bifurcation diagram; (b) LEs.

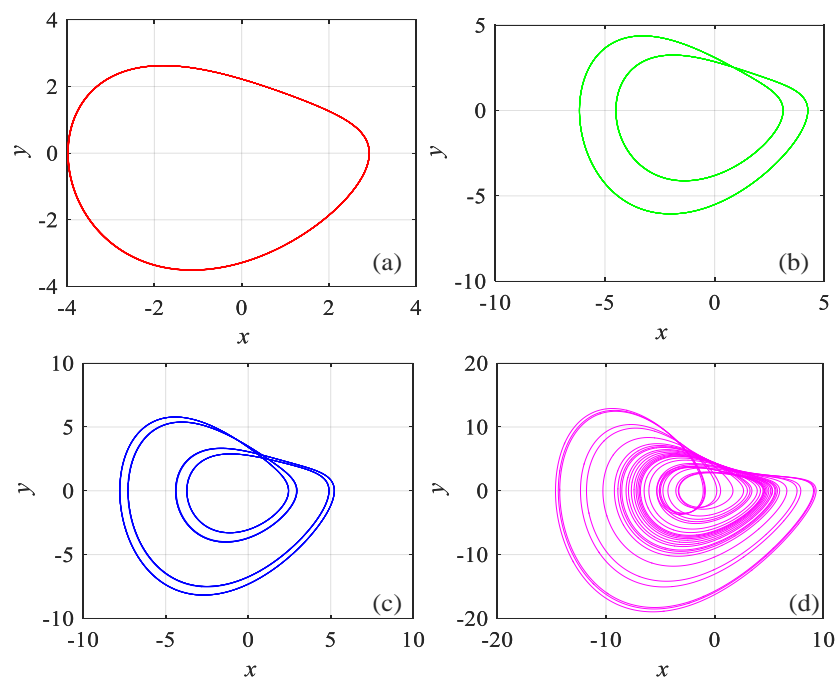


Figure 3. Phase diagrams of the system with $c = 1$, $e = 0.5$, and different b . (a) $b = 0.7$; (b) $b = 0.818$; (c) $b = 0.88$; (d) $b = 1$.

Fix $b = 1$, $e = 0.5$, and vary c from 1 to 1.3 with a step size of 0.0012. Bifurcation diagrams and the corresponding LEs with the variation of parameter c are shown in Figure 4. According to Figure 4, the bifurcation is period-doubling with the decrease of parameter c , and the system becomes chaotic when $c < 1.1$. Meanwhile, phase diagrams of the system with $b = 1$, $e = 0.5$, and different c , including $c = 1.05$, $c = 1.1$, $c = 1.15$, and $c = 1.3$, are shown in Figure 5. It shows that the system has different states with different parameter c .

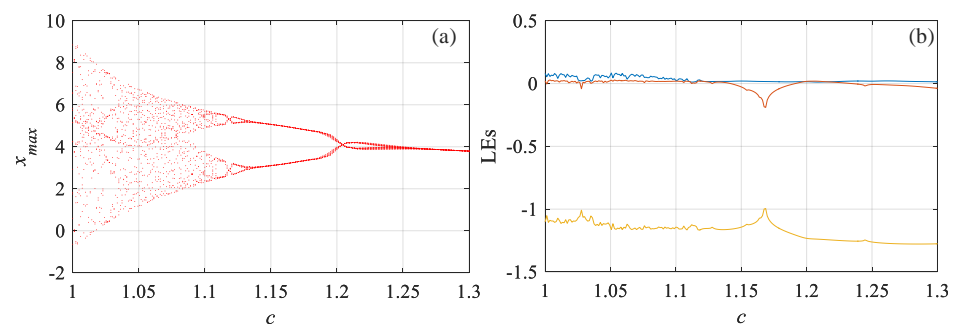


Figure 4. Dynamics of the memristor-based jerk system with the parameter c . (a) bifurcation diagram; (b) LEs.

According to the above dynamical analysis, it shows that the system has rich dynamics with the variation of parameters b and c . The system is chaotic when the parameters b and c take values near one, while the system becomes too periodic with the decrease of b and the increase of c . In the next section, the complexity of the system is analyzed by employing the multiscale sample entropy (MSampEn) algorithm.

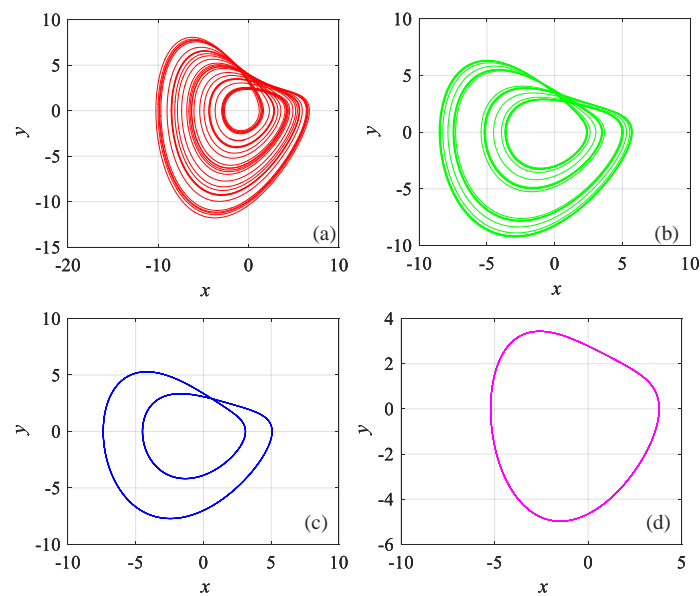


Figure 5. Phase diagrams of the system with $b = 1$, $e = 0.5$, and different c . (a) $c = 1.05$; (b) $c = 1.1$; (c) $c = 1.15$; (d) $c = 1.3$.

3.1.2. Complexity Analysis

SampEn [23] is a complexity measure for nonlinear time series. When the measure result is larger, the complexity of the time series is higher, which means that the original system is more complex. The SampEn of a nonlinear time series can be estimated by the following steps.

Step 1: For a given time series $\{x(i), i = 0, 1, 2, \dots, N-1\}$ of length N and embedding dimension m , the m -dimensional phase-space reconstruction is expressed as:

$$X(i) = [x(i), x(i+1), \dots, x(i+m-1)], \quad (13)$$

where $i = 0, 1, 2, \dots, N-m$.

Step 2: Define the Euclidean distance between the vector $X(i)$ and vector $X(j)$ as:

$$d[X(i), X(j)] = \max_{k=0 \rightarrow m-1} \{|X(i+k) - X(j+k)|\}. \quad (14)$$

Step 3: For a given similarity r , count the number of $d[X(i), X(j)] < r$, where $i = 0, 1, 2, \dots, N-m$, $j = 0, 1, 2, \dots, N-m$, and $i \neq j$. If $d[X(i), X(j)] < r$, then $\phi_r^m(i, j) = 0$; otherwise, $\phi_r^m(i, j) = 0$. The average value of $\phi_r^m(i)$ can be calculated as:

$$\phi^m(i) = \frac{1}{N-m} \sum_{j=0, i \neq j}^{N-m} \phi_r^m(i, j). \quad (15)$$

Then, we have:

$$\Phi^m(r) = \frac{1}{N-m+1} \sum_{i=0}^{N-m} \phi^m(i). \quad (16)$$

Step 4: Similarly, change m to $m+1$, repeat steps one to three, and obtain $\Phi^{m+1}(r)$. Then, SampEn is defined as [23,25]:

$$\text{SampEn}(m, r, x) = -\ln \frac{\Phi^{m+1}(r)}{\Phi^m(r)}. \quad (17)$$

In this paper, we set $m = 2$ and $r = 0.2SD$, where SD means the standard deviation of the original time series.

Based on the SampEn algorithm, MSampEn is described as follows.

Step 1: For a one-dimensional time sequence $\{x(i), i = 0, 1, 2, \dots, N-1\}$ of length N , its coarse-grained time series under scale factor τ is constructed as [25]:

$$Y^\tau(i, j) = x(i + \tau \cdot (j - 1)), \quad (18)$$

where $j = 0, 1, 2, \dots, N-1, 1 \leq j \leq [N/\tau]$, and $[\cdot]$ denotes the floor function.

Step 2: MSampEn is calculated by:

$$MSampEn(x, \tau) = \frac{1}{15} \sum_{\tau=11}^{25} SampEn(m, r, Y^\tau(i, :)). \quad (19)$$

The complexity of the jerk system is analyzed and the analysis results are illustrated in Figures 6 and 7.

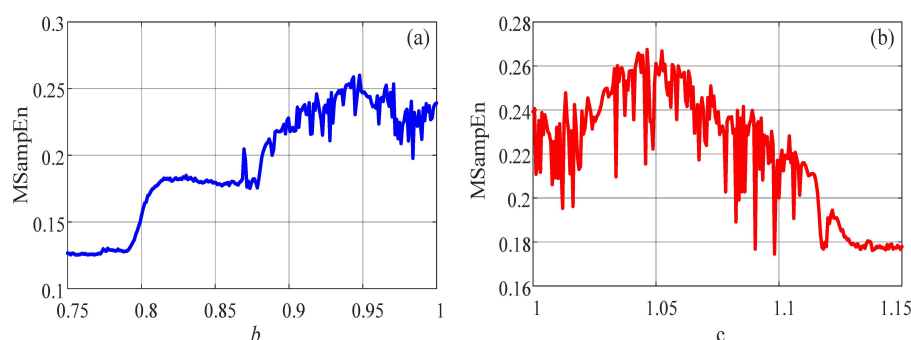


Figure 6. MSampEn complexity of the system with different parameters. (a) the parameter b varying; (b) the parameter c varying.

Firstly, the complexity of the system with the variation of parameters b and c are estimated, and the results are shown in Figure 6a,b, respectively. For Figure 6a, $c = 1$, $e = 0.5$, and vary b from 0.4 to 1 with a step size of 0.0024, while for Figure 6b, $b = 1$, $e = 0.5$, and vary c from 1 to 1.3 with a step size of 0.0012. This shows that the high complexity intervals of the system are $b \in [0.9, 1]$ and $c \in [1, 1.1]$. Obviously, the trend of the MSampEn analysis results match well with the corresponding Lyapunov exponents, but it is more intuitional. For the real encryption applications, one can choose system parameters when the system has a MSampEn estimate value larger than 0.2.

Secondly, let $e = 0.1$, b vary from 0.75 to 1 with a step size of 0.0025, and c vary from 1 to 1.15 with a step size of 0.0015; the complexity analysis result in the parameter plane b - c is illustrated in Figure 7. Thus, we have an overall view of the high complexity region of the jerk system, and it shows that the system has high complexity in the top left corner of the parameter plane.

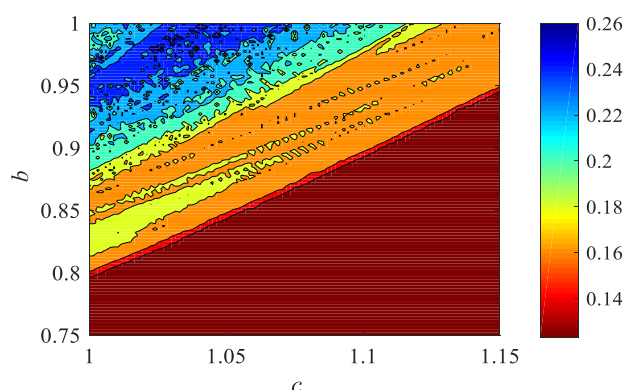


Figure 7. MSampEn complexity of the system in the parameter plane b - c .

3.2. Circuit Implementation

It is important to realize the system in the hardware to verify the existence of chaos. In this section, circuit implementation of the proposed jerk system is carried out.

3.2.1. Circuit Design of the Memristor

The circuit of the memristor is shown in Figure 8, where $R_{m1} = R_{m4} = 10 \text{ K}\Omega$, $R_{m2} = R_{m3} = 20 \text{ K}\Omega$ and $C_{m1} = 100 \text{ nF}$. The operational amplifier is AD711KN, the multiplier is AD633JN, and the operation voltage is $\pm 15 \text{ V}$. According to Figure 8, the port characteristics can be described by the following equation:

$$\begin{cases} h(t) = -\frac{R_{m4}}{R_{m2}}x(t)y(t) - \frac{R_{m4}}{R_{m3}}y(t) \\ \dot{x}(t) = -\frac{R_{m4}}{R_{m1}C_{m1}}y(t) \end{cases} \quad (20)$$

Meanwhile, the voltage–current characteristic curves of the port for the memristor are shown in Figure 9. Obviously, it shows the “8”-shaped curve, which indicates that the realized circuit is a equivalent circuit of the memristor. Moreover, it shows that there exists a memristor in the proposed jerk system.

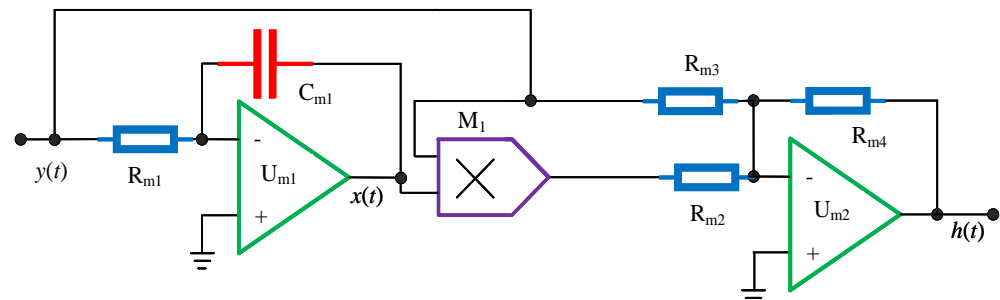


Figure 8. Circuit of the generalized memristor.

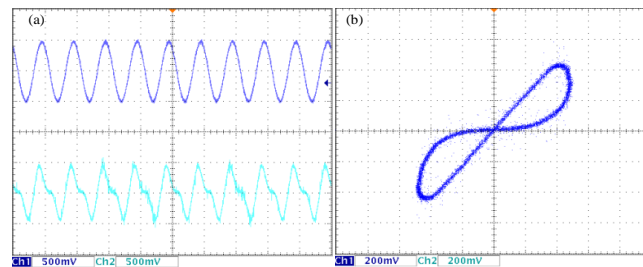


Figure 9. The voltage–current characteristic curves of the port for the memristor. (a) time series; (b) V–I curve.

3.2.2. Hardware Circuit Implementation of the Jerk System

The chaotic system is realized in the hardware circuit, and the jerk chaotic circuit with memristor function is shown in Figure 10, where the electronic components in the shadow area provide the function of a memristor, and U_3 is the reverse proportional operational amplifier. As a result, the equations of the circuit are given by:

$$\begin{cases} \dot{x} = \frac{y}{R_1C_1} \\ \dot{y} = \frac{z}{R_2C_2} \\ \dot{z} = -\frac{z}{R_3C_3} - \frac{x}{R_8C_3} - \frac{1}{C_3} \left(-\frac{1}{R_7}xy + \frac{R_5}{R_4R_6}y \right) \end{cases} \quad (21)$$

The experimental platform is given in Figure 11. When $R_1 = R_2 = R_3 = R_5 = R_6 = R_8 = 10 \text{ k}\Omega$, $R_4 = R_7 = 20 \text{ k}\Omega$, $C_1 = C_2 = C_3 = 100 \text{ nF}$. The operational amplifier is AD711KN, the multiplier is AD633JN, and the operation voltage is $\pm 15 \text{ V}$. The chaotic attractors obtained are shown in Figure 12.

The designed circuit contains the memristor circuit, as shown in Figure 10, but it has a resistance R_8 and a capacitance C_3 connected with it; thus, it does not work like the usual-sense nonlinear memristor circuit. Moreover, the chaotic analog circuits can generate real chaos while the corresponding digital implementation has the finite precision effect. For computer software (Multisim, Spice, and Psim)-based analog circuit simulations, they are essentially another kind of digital results. Generally, digital solutions and analog solutions should agree well with each other since they are both models of the original systems. In the next section, we will give an in-depth exploration of the difference between a “memristor chaotic system” and a “chaotic system with memristor function”.

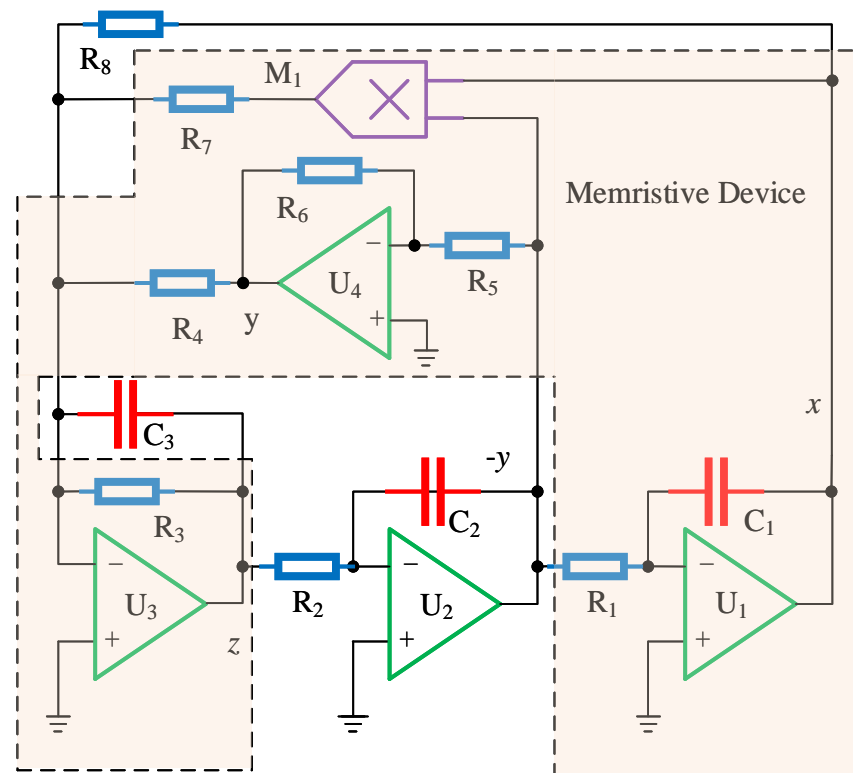


Figure 10. The jerk chaotic circuit with memristor function.

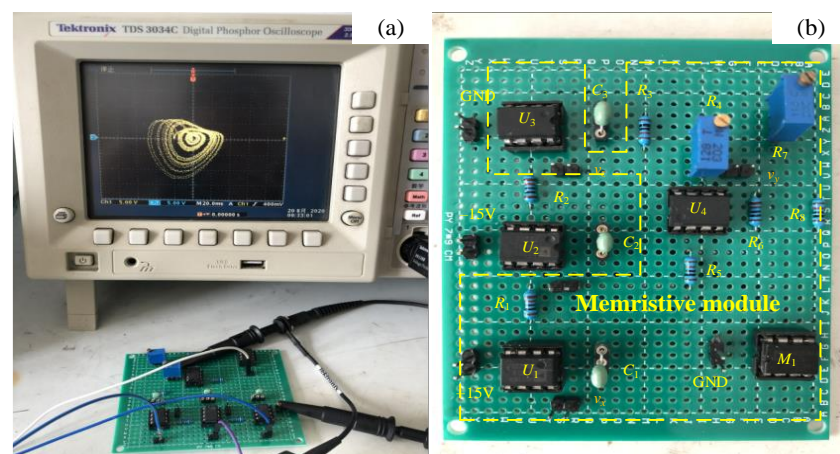


Figure 11. The experimental platform. (a) results in the oscilloscope; (b) the realized real circuit.

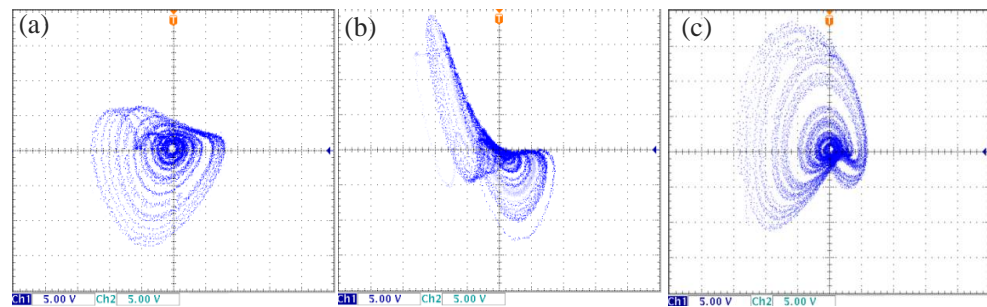


Figure 12. Phase diagrams captured from the real circuit. (a) x–y plane; (b) x–z plane; (c) y–z plane.

4. Nonlinear Systems with Memristor

4.1. Modeling Using the Generalized Memristor

In fact, there many nonlinear systems can be modeled based on the generalized memristor. However, some issues should be discussed. Firstly, two more examples are presented. The first example is that the proposed jerk system can also be modeled by another memristor, which is:

$$\begin{cases} h = exy \\ \dot{x} = y \end{cases}, \quad (22)$$

and the system is given by:

$$\begin{cases} \dot{x} = y \\ \dot{y} = z \\ \dot{z} = -bx - cz - ey + h \end{cases}. \quad (23)$$

Although the modeling is different, the final circuit is the same as is shown in Figure 10. The second example is the Lorenz system, which can be modeled by a generalized memristor. Here, we take the simplified Lorenz system [26] as an example of the system modeling process. The system is given by:

$$\begin{cases} \dot{x} = 10(y - x) \\ \dot{y} = (24 - 4c)x - xz + cy \\ \dot{z} = xy - 8z/3 \end{cases} \quad (24)$$

According to the definition of the generalized memristor, the system contains a generalized memristor, which is defined by:

$$\begin{cases} \dot{x} = 10(y - x) \\ h = xy \end{cases}. \quad (25)$$

Remark 1. Suppose that $x(t)$ and $y(t)$ are the state variables of the nonlinear differential equation, and we have $\dot{x}(t) = f(x, y, t)$; if the system has an item $g(x, y, t)y(t)$ in another equation of the system, the system can be modeled by using the generalized memristor.

However, it should be noted that this kind of modeling of nonlinear systems is not the natural way for the real memristor-based system. As we can see, the state variable x is the internal states of the memristor; it is not reasonable for it to act as a variable in the system, except in the memristive system. For those systems, they indeed have a memristor in the circuit; however, the so-called memristor only has the function of a memristor.

Remark 2. In those memristor-based jerk systems, the memristor is defined by:

$$\begin{cases} h(t) = g(x)y \\ \dot{x} = y \end{cases}. \quad (26)$$

Obviously, $\dot{x} = y$ is one of the equations of the jerk system, and $g(x)y$ belongs to the nonlinear function of the jerk system.

Remark 3. There are many chaotic systems, for example, the Lorenz system, that contain generalized memristors.

Remark 4. The output and input of the generalized memristor circuit in the above nonlinear systems could not be the voltage and current pair, but could be voltage and voltage pair or current and current pair. This depends on how the circuit of the generalized memristor is designed.

Remark 5. Suppose that a nonlinear system can satisfy the following three rules; then, the system could be realized by the memristor element theoretically. The three rules are: (1) it has an equation given by $\dot{x}(t) = f(x, y, t)$; (2) there is only an item $g(x, y, t)y(t)$ in one of the other equations; (3) the variable “ x ” should not be observed in the system, except $f(x, y, t)$ and $g(x, y, t)y(t)$.

Suppose that there is a nonlinear system which is defined by:

$$\begin{cases} \dot{x} = ay \\ \dot{y} = -b(x + g(z)y) \\ \dot{z} = f(y, z) \end{cases} \quad (27)$$

where $\begin{cases} h(t) = -g(z)y \\ \dot{z} = f(y, z) \end{cases}$ is the generalized memristor, and $g(z)$ and $f(y, z)$ are the nonlinear functions.

According to Remark 5, the internal state variable z only exists in the generalized memristor; thus, this system can be designed by the memristor circuit and the resulting circuit is given by Figure 13. According to the Kirchhoff law, the nonlinear function of the circuit is given by:

$$\begin{cases} \frac{dV_c}{dt} = \frac{1}{C}i_L \\ \frac{di_L}{dt} = -\frac{1}{L}[V_c - g(z)i_M] \\ \frac{dz}{dt} = \tilde{f}(i_M, z) \end{cases} \quad (28)$$

where $\tilde{f}(i_M, z) = f(i_L, z)$. If we let $V_c = x$, $i_L = y$, $i_M = -y$, $a = 1/C$, and $b = 1/L$, we can obtain the target system. Since the equations $g(z)$ and $\tilde{f}(i_M, z)$ have many different choices, Equation (26) has many different kinds of forms. For instance, B. Muthuswamy et al. [27] analyzed different kinds of nonlinear systems based on this circuit. Moreover, let us check the proposed jerk system; if $b = 0$, then it can be realized using a memristor. Otherwise, its circuit cannot be realized by using the memristor device since there is an item $-bx$.

Moreover, the Lorenz system contains the memristor function $\begin{cases} \dot{x} = 10(y - x) \\ \dot{y} = xy \end{cases}$, but it has items containing “ x ” in each of the equations. Thus, it cannot be realized using the memristor device. In conclusion, some of the nonlinear systems can be designed based on the memristor element.

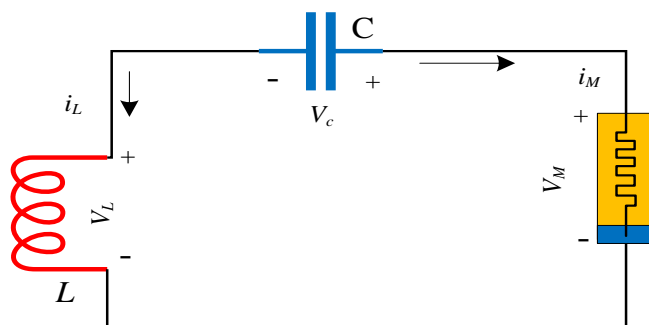


Figure 13. A memristor circuit for the nonlinear system.

As shown in the above analysis, it illustrates two methods for the circuit design of nonlinear systems. Namely, the first method is to design a memristor circuit or to introduce a memristor to the system, while the second method is to make the system contain a memristor function. Essentially, the circuit of the nonlinear system from method one is still same as the traditional method, while the second method uses the memristor electron component to realize the system. However, the second method has more limitations.

4.2. Further Discussions

Firstly, there are many different kinds of memristors proposed in the existing references. Table 1 summarizes some memristors with different kinds of equations, such as piecewise-linear nonlinearity, absolute value, linear function, sine function, and square function. Meanwhile, the Known memristor is also considered for comparison. The $i-v$ hysteresis loops observed in the Known memristor are not as smooth as those that are simulated.

Table 1. The characters of different kinds of memristors.

Type	Reference	Equations
Piecewise-linear	Ref. [28]	$M(q) = \frac{dq(q)}{dq} = \begin{cases} a, & q < 1 \\ b, & q > 1 \end{cases}$
Absolute value	Ref. [29]	$\begin{cases} i(t) = W(\varphi)v(t) \\ W(\varphi) = -a + b \varphi(t) \\ \dot{\varphi}(t) = v(t) \end{cases}$
Linear function	Ref. [30]	$\begin{cases} \dot{x}_1(t) = x_2(t) \\ h(t) = [x_1(t) - 1]x_2(t) \end{cases}$
	Ref. [31]	$\begin{cases} \dot{x} = u_m \\ f_m = (1+x)u_m \end{cases}$
Sine function	Ref. [32]	$W(\varphi) = dq(\varphi)/d\varphi = \cosh(\varphi)$
Square function	Ref. [33]	$W(\varphi) = dq(\varphi)/d\varphi = a + 3b\varphi^2$
	Ref. [34]	$\begin{cases} \dot{x} = y \\ h = (x^2 - 2)y \end{cases}$
	Ref. [35]	$\begin{cases} i = \alpha z^2 v \\ \dot{z} = -\beta v - \lambda z + kvz \end{cases}$
Cubic function	Ref. [36]	$g(v_R) = a_0 + av_R + bv_R^2 + cv_R^3$
Higher-order	Ref. [37]	$q(\phi) = a\phi^5 + b\phi^3 + c\phi + d$
Known memristor	Ref. [38]	$G(\phi) = \frac{\phi}{R_{ON}} + \frac{1-\phi}{R_{OFF}}$, fitted curve
	Ref. [39]	$i-v$ characteristic curves presented

Generally, those memristors can be defined by:

$$\begin{cases} h(t) = g(x)y \\ \dot{x} = f(y) \end{cases}, \quad (29)$$

which means the ideal memristor. The main consideration to use this kind of “simple” memristor is to simplify the circuit implementation in real applications. However, a few memristors are defined by:

$$\begin{cases} h(t) = g(x)y \\ \dot{x} = f(x, y) \end{cases}. \quad (30)$$

For example, Ref. [35] proposed a memristor which is defined in this form.

Table 2 shows some similar jerk systems which also contain memristors. Those systems have a similar structure to the system proposed in this paper. Since the variable x or x_1 also appears in the third equation of those systems, according to Remark 2, those systems cannot be realized using a memristor device related to the given memristor functions.

Table 2. Nonlinear systems with memristor functions.

Reference	System Proposed	Memristor Function
Ref. [19]	$\begin{cases} \dot{x} = y \\ \dot{y} = z \\ \dot{z} = -ax - cz + y^2 + h \end{cases}$	$\begin{cases} h = b(x-1)y \\ \dot{x} = y \end{cases}$
Ref. [40]	$\begin{cases} \dot{x} = y \\ \dot{y} = z \\ \dot{z} = -x - z + h \end{cases}$	$\begin{cases} h = (1-x^2)y \\ \dot{x} = y \end{cases}$
Ref. [41]	$\begin{cases} \dot{x} = y \\ \dot{y} = z \\ \dot{z} = -bx - z + h \end{cases}$	$\begin{cases} h = (a-x^2)y \\ \dot{x} = y \end{cases}$

Table 3 shows nonlinear systems with memristor devices, where the systems have the same memristor function. According to Remark 2, those systems can be realized using the memristor device. In fact, those systems are realized using an analog circuit [42–44]. Firstly, there is an item “ $W(x_4)x_1$ ” or “ $W(\omega)x$ ”, which contains the memristor function. Secondly, the variable x_4 or ω just appears in the function $W(\cdot)$. Thirdly, although the memristor functions are the same, defined by $W(\varphi) = a + 3b\varphi^2$, those systems are different. The system in Ref. [42] is proposed based on the Lorenz system, the system in Ref. [43] is designed based on Chua’s system, while the system in Ref. [44] is derived from a memristor circuit. As a result, it shows that there are many different kinds of memristor systems.

Table 3. Nonlinear systems with memristor devices.

Reference	System Proposed
Ref. [42]	$\begin{cases} \dot{x} = \alpha(y-x) \\ \dot{y} = -xz + \beta y - \rho W(\omega)x \\ \dot{z} = xy - \gamma z \\ \dot{\omega} = x \end{cases}$
Ref. [43]	$\begin{cases} \dot{x}_1 = \alpha[x_2 - x_1 + \varepsilon x_1 - W(x_4)x_1] \\ \dot{x}_2 = x_1 - x_2 + x_3 \\ \dot{x}_3 = -\beta x_2 \\ \dot{x}_4 = x_1 \end{cases}$
Ref. [44]	$\begin{cases} \dot{x} = \alpha(z - W(\omega)x) \\ \dot{y} = \beta y - z \\ \dot{z} = y - x - \xi z \\ \dot{\omega} = x \end{cases}$

Until now, memristor-based nonlinear systems have been widely investigated. This paper indicates the fact that there exist two kinds of memristor-based nonlinear systems, namely, nonlinear systems with a memristor device and nonlinear systems with a memristor equation. Of course, those nonlinear systems with a memristor device have memristor equations. The main difference is that the nonlinear systems with a memristor device can be realized using a memristor device, while nonlinear systems with a memristor equation cannot be. As far as we know, there are many systems that contain memristor equations. How to investigate the effect of those memristor equations to the dynamics of nonlinear systems merits further discussion.

5. Conclusions

In this paper, a new jerk system which contains a memristor function is proposed and analyzed. The characteristics of the memristor and the dynamics of the jerk system are investigated. It shows that the proposed generalized memristor satisfies the definition of the memristor, and that the jerk system has rich dynamical behaviours. The operational amplifiers and multipliers are used to construct the hardware circuit of the memristor and the proposed jerk system. The realization results show that the memristor can generate the

“8”-shaped pinched hysteresis loops, and chaotic attractors are observed in the oscilloscope. Compared with the circuit designed in other references, the circuit in this paper is simpler since it has fewer electronic components. Finally, we found that there are many nonlinear systems that contain memristor equations, but not all of them can be realized using the memristor device. As for future work, we hold the opinion that there are two aspects which deserve further study. The first aspect is to find more systems to explore the boundary between the nonlinear systems and the generalized memristors. The second is to discuss the relationship between the nonlinearity of the system and nonlinearity in the memristor equation.

Author Contributions: Conceptualization, X.W. and S.H.; methodology, X.W.; software, W.T.; validation, H.W., S.H. and X.W.; formal analysis, S.H.; investigation, H.W.; resources, W.T.; data curation, S.H.; writing—original draft preparation, S.H.; writing—review and editing, X.W. and H.W.; visualization, W.T.; supervision, S.H.; project administration, S.H.; funding acquisition, X.W. All authors have read and agreed to the published version of the manuscript.

Funding: This work was supported by the Natural Science Foundation of China (Nos. 62061008, 61901530, 62071496), the Natural Science Foundation of Hunan Province (No. 2020JJ5767), the Science and Technology Foundation of Guizhou Province of China (No. [2018]1115), the Science and Technology Plan Project of Guizhou Province of China (No. [2018]5769), and the Doctoral Scientific Research Foundation of Guizhou Normal University (2017).

Institutional Review Board Statement: Not applicable.

Informed Consent Statement: Not applicable.

Data Availability Statement: All data and models during the study appear in the submitted article.

Acknowledgments: The authors would like to thank the three anonymous reviewers for their constructive comments and insightful suggestions.

Conflicts of Interest: The authors declare no conflict of interest.

References

1. Chua, L. Memristor-the missing circuit element. *IEEE Trans. Circuit Theory* **1971**, *18*, 507–519. [\[CrossRef\]](#)
2. Chua, L.O.; Kang, S.M. Memristive devices and systems. *Proc. IEEE* **1976**, *64*, 209–223. [\[CrossRef\]](#)
3. Strukov, D.; Snider, G.S.; Stewart, D.; Williams, R. The missing memristor found. *Nature* **2008**, *453*, 80–83. [\[CrossRef\]](#)
4. Lai, Q.; Wan, Z.; Kuate, P.D.K.; Fotsin, H. Coexisting attractors, circuit implementation and synchronization control of a new chaotic system evolved from the simplest memristor chaotic circuit. *Commun. Nonlinear Sci. Numer. Simul.* **2020**, *89*, 105341. [\[CrossRef\]](#)
5. Rajagopal, K.; Vaidyanathan, S.; Karthikeyan, A.; Srinivasan, A. Complex novel 4D memristor hyperchaotic system and its synchronization using adaptive sliding mode control. *Alex. Eng. J.* **2018**, *57*, 683–694. [\[CrossRef\]](#)
6. Siddik, A.; Haldar, P.K.; Garu, P.; Bhattacharjee, S.; Das, U.; Barman, A.; Roy, A.; Sarkar, P. Enhancement of data storage capability in a bilayer oxide-based memristor for wearable electronic applications. *J. Phys. D* **2020**, *53*, 295103. [\[CrossRef\]](#)
7. Kim, H.; Sah, M.P.; Yang, C.; Roska, T.; Chua, L.O. Memristor bridge synapses. *Proc. IEEE* **2011**, *100*, 2061–2070. [\[CrossRef\]](#)
8. Li, C.; Belkin, D.; Li, Y.; Yan, P.; Hu, M.; Ge, N.; Jiang, H.; Montgomery, E.; Lin, P.; Wang, Z.; et al. Efficient and self-adaptive in-situ learning in multilayer memristor neural networks. *Nat. Commun.* **2018**, *9*, 1–8. [\[CrossRef\]](#)
9. He, S.; Sun, K.; Peng, Y.; Wang, L. Modeling of discrete fracmemristor and its application. *AIP Adv.* **2020**, *10*, 015332. [\[CrossRef\]](#)
10. Peng, Y.; He, S.; Sun, K. A higher dimensional chaotic map with discrete memristor. *AEU-Int. J. Electron. Commun.* **2021**, *129*, 153539. [\[CrossRef\]](#)
11. Sprott, J.C. A new chaotic jerk circuit. *IEEE Trans. Circuits Syst. II Express Briefs* **2011**, *58*, 240–243. [\[CrossRef\]](#)
12. Vaidyanathan, S. Analysis, adaptive control and synchronization of a novel 4-D hyperchaotic hyperjerk system via backstepping control method. *Arch. Control Sci.* **2016**, *26*, 311–338. [\[CrossRef\]](#)
13. Kengne, J.; Njitacke, Z.; Nguomkam Negou, A.; Fouodji Tsostop, M.; Fotsin, H.B. Coexistence of multiple attractors and crisis route to chaos in a novel chaotic jerk circuit. *Int. J. Bifurc. Chaos* **2016**, *26*, 1650081. [\[CrossRef\]](#)
14. Sabarathinam, S.; Volos, C.K.; Thamilmaran, K. Implementation and study of the nonlinear dynamics of a memristor-based Duffing oscillator. *Nonlinear Dyn.* **2017**, *87*, 37–49. [\[CrossRef\]](#)
15. Volos, C.; Akgul, A.; Pham, V.T.; Stouboulos, I.; Kyprianidis, I. A simple chaotic circuit with a hyperbolic sine function and its use in a sound encryption scheme. *Nonlinear Dyn.* **2017**, *89*, 1047–1061. [\[CrossRef\]](#)
16. Bao, H.; Wang, N.; Bao, B.; Chen, M.; Jin, P.; Wang, G. Initial condition-dependent dynamics and transient period in memristor-based hypogenetic jerk system with four line equilibria. *Commun. Nonlinear Sci. Numer. Simul.* **2018**, *57*, 264–275. [\[CrossRef\]](#)

17. Kengne, J.; Negou, A.N.; Tchiotso, D. Antimonotonicity, chaos and multiple attractors in a novel autonomous memristor-based jerk circuit. *Nonlinear Dyn.* **2017**, *88*, 2589–2608. [\[CrossRef\]](#)
18. Hua, M.; Yang, S.; Xu, Q.; Chen, M.; Wu, H.; Bao, B. Forward and reverse asymmetric memristor-based jerk circuits. *AEU-Int. J. Electron. Commun.* **2020**, *123*, 153294. [\[CrossRef\]](#)
19. Wang, Z.; Sun, W.; Wei, Z.; Zhang, S. Dynamics and delayed feedback control for a 3D jerk system with hidden attractor. *Nonlinear Dyn.* **2015**, *82*, 577–588. [\[CrossRef\]](#)
20. Zhang, Y.; Liu, Z.; Wu, H.; Chen, S.; Bao, B. Extreme multistability in memristive hyper-jerk system and stability mechanism analysis using dimensionality reduction model. *Eur. Phys. J. Spec. Top.* **2019**, *228*, 1995–2009. [\[CrossRef\]](#)
21. He, S.; Sun, K.; Peng, Y. Detecting chaos in fractional-order nonlinear systems using the smaller alignment index. *Phys. Lett. A* **2019**, *383*, 2267–2271. [\[CrossRef\]](#)
22. Lai, Q.; Kuate, P.D.K.; Liu, F.; Lu, H.H.C. An extremely simple chaotic system with infinitely many coexisting attractors. *IEEE Trans. Circuits Syst. II Express Briefs* **2019**, *67*, 1129–1133. [\[CrossRef\]](#)
23. Šupová, M. The Significance and Utilisation of Biomimetic and Bioinspired Strategies in the Field of Biomedical Material Engineering: The Case of Calcium Phosphat—Protein Template Constructs. *Materials* **2020**, *13*, 327. [\[CrossRef\]](#) [\[PubMed\]](#)
24. Adhikari, S.P.; Sah, M.; Kim, H.; Chua, L. Three Fingerprints of Memristor. *IEEE Trans. Circuits Syst. I Regul. Pap.* **2013**, *60*, 3008–3021. [\[CrossRef\]](#)
25. Yang, Z.X.; Zhong, J.H. A hybrid EEMD-based SampEn and SVD for acoustic signal processing and fault diagnosis. *Entropy* **2016**, *18*, 112. [\[CrossRef\]](#)
26. Sun, K.; Wang, X.; Sprott, J.C. Bifurcations and chaos in fractional-order simplified Lorenz system. *Int. J. Bifurc. Chaos* **2010**, *20*, 1209–1219. [\[CrossRef\]](#)
27. Muthuswamy, B.; Chua, L.O. Simplest chaotic circuit. *Int. J. Bifurc. Chaos* **2010**, *20*, 1567–1580. [\[CrossRef\]](#)
28. Itoh, M.; Chua, L.O. Memristor oscillators. *Int. J. Bifurc. Chaos* **2008**, *18*, 3183–3206. [\[CrossRef\]](#)
29. Bao, B.; Jiang, P.; Wu, H.; Hu, F. Complex transient dynamics in periodically forced memristive Chua's circuit. *Nonlinear Dyn.* **2015**, *79*, 2333–2343. [\[CrossRef\]](#)
30. Bao, B.; Zou, X.; Liu, Z.; Hu, F. Generalized memory element and chaotic memory system. *Int. J. Bifurc. Chaos* **2013**, *23*, 1350135. [\[CrossRef\]](#)
31. Prousalis, D.A.; Volos, C.K.; Stouboulos, I.N.; Kyprianidis, I.M. A hyperjerk memristive system with infinite equilibrium points. *AIP Conf. Proc.* **2017**, *1872*, 020024.
32. Zhulin, W.; Fuhong, M.; Guangya, P.; Yaoda, W.; Yi, C. Bifurcation and Chaos of the Memristor Circuit. *Int. J. Comput. Inf. Eng.* **2016**, *10*, 1976–1982.
33. Bao, B.; Liu, Z.; Xu, J. Steady periodic memristor oscillator with transient chaotic behaviours. *Electron. Lett.* **2010**, *46*, 237–238. [\[CrossRef\]](#)
34. Feng, W.; He, Y.G.; Li, C.L.; Su, X.M.; Chen, X.Q. Dynamical behavior of a 3D jerk system with a generalized Memristive device. *Complexity* **2018**, *2018*, 5620956. [\[CrossRef\]](#)
35. Wu, R.; Wang, C. A new simple chaotic circuit based on memristor. *Int. J. Bifurc. Chaos* **2016**, *26*, 1650145. [\[CrossRef\]](#)
36. Zhong, G.Q. Implementation of Chua's circuit with a cubic nonlinearity. *IEEE Trans. Circuits Syst. I Fundam. Theory Appl.* **1994**, *41*, 934–941. [\[CrossRef\]](#)
37. Wang, C.; Xia, H.; Zhou, L. Implementation of a new memristor-based multiscroll hyperchaotic system. *Pramana* **2017**, *88*, 34. [\[CrossRef\]](#)
38. Ostrovskii, V.; Fedoseev, P.; Bobrova, Y.; Butusov, D. Structural and Parametric Identification of Known Memristors. *Nanomaterials* **2021**, *12*, 63. [\[CrossRef\]](#)
39. Volos, C.; Nistazakis, H.; Pham, V.T.; Stouboulos, I. The first experimental evidence of chaos from a nonlinear circuit with a real memristor. In Proceedings of the 2020 9th International Conference on Modern Circuits and Systems Technologies (MOCAST), Bremen, Germany, 7–9 September 2020; pp. 1–4.
40. Ding, Y.; Zhang, Q. Impulsive homoclinic chaos in Van der Pol Jerk system. *Trans. Tianjin Univ.* **2010**, *16*, 457–460. [\[CrossRef\]](#)
41. Sanjaya, W.; Anggraeni, D.; Denya, R.; Ismail, N. Numerical Simulation Bidirectional Chaotic Synchronization of Spiegel-Moore Circuit and Its Application for Secure Communication. *IOP Conf. Ser. Mater. Sci. Eng.* **2017**, *180*, 012066 [\[CrossRef\]](#)
42. Li, Q.; Zeng, H.; Li, J. Hyperchaos in a 4D memristive circuit with infinitely many stable equilibria. *Nonlinear Dyn.* **2015**, *79*, 2295–2308. [\[CrossRef\]](#)
43. Rocha, R.; Ruthiramoorthy, J.; Kathamuthu, T. Memristive oscillator based on Chua's circuit: Stability analysis and hidden dynamics. *Nonlinear Dyn.* **2017**, *88*, 2577–2587. [\[CrossRef\]](#)
44. Peng, G.; Min, F. Multistability analysis, circuit implementations and application in image encryption of a novel memristive chaotic circuit. *Nonlinear Dyn.* **2017**, *90*, 1607–1625. [\[CrossRef\]](#)